

## Kinetics of the Reaction of OH Radicals with CH<sub>2</sub>ClCF<sub>2</sub>Cl and CH<sub>2</sub>ClCF<sub>3</sub> over an Extended Temperature Range

Tunchen D. Fang,<sup>†</sup> Philip H. Taylor,<sup>\*,‡</sup> and Rajiv J. Berry<sup>§</sup>

Physical Optics Corporation, 2545 W. 237th Street, Suite B, Torrance, California 90505-5228, Environmental Sciences and Engineering Group, University of Dayton Research Institute, 300 College Park, Dayton, Ohio 45469-0132, and Center for Computational Modeling of Nonstructural Materials, WL/MLBT, Wright-Patterson AFB, Ohio 45433

Received: October 29, 1998; In Final Form: February 22, 1999

Rate coefficients are reported for the gas-phase reaction of hydroxyl (OH) radicals with CH<sub>2</sub>ClCF<sub>2</sub>Cl ( $k_1$ ) and CH<sub>2</sub>ClCF<sub>3</sub> ( $k_2$ ) over an extended temperature range. The measurements were performed using a laser photolysis/laser-induced fluorescence (PLP/LIF) technique under slow flow conditions at a total pressure of  $740 \pm 10$  Torr. The lower temperature measurements for  $k_1$  were in agreement with previous measurements using different techniques. Prior measurements for  $k_2$  using different techniques exhibit significant scatter. The new lower temperature data reported here lie intermediate to the previous measurements. Arrhenius plots of the data exhibit significant curvature and were fit to the expression  $k(T) = AT^B \exp(-C/T)$ . A semiempirical fitting approach was used in which  $A$  and  $B$  were obtained from transition-state theory (TST) and  $C$  was determined from a nonlinear least-squares fit to the experimental data. Ab initio calculations were used to evaluate the thermochemical properties of the activated complex. The resulting modified Arrhenius expressions were  $k_1(295-788 \text{ K}) = (8.53 \pm 4.06) \times 10^{-19} T^{2.28 \pm 0.18} \exp[(-937 \pm 296)/T] \text{ cm}^3 \text{ molecule}^{-1} \text{ s}^{-1}$  and  $k_2(295-866 \text{ K}) = (3.06 \pm 4.02) \times 10^{-18} T^{1.91 \pm 0.03} \exp[(-644 \pm 313)/T] \text{ cm}^3 \text{ molecule}^{-1} \text{ s}^{-1}$ . Error limits are  $\pm 2\sigma$ . The TST-based modified Arrhenius expression is compared to previous TST and SAR predictions. The effect of halogen substitution on the reactivity of these compounds is briefly discussed. The incorporation of a Wigner tunneling factor and its impact on the TST fit of the data is also presented and discussed.

### Introduction

The fate of anthropogenic halogenated hydrocarbons that are released to the atmosphere in the course of various industrial or technological activities is of great environmental concern. In addition to their well-known connection to stratospheric ozone destruction, these compounds are effective greenhouse gases. The present policy (Montreal protocol) is to replace all perhalogenated Freons and Halons with compounds that have some hydrogen ligands. Hydrochlorofluorocarbons (HCFCs) are readily attacked by oxidizing agents in the lower atmosphere or in combustion systems, so their lifetimes are much shorter and their ozone-depleting and global-warming potentials are correspondingly reduced.

The fastest process contributing to the destruction of halogenated hydrocarbons, both under atmospheric conditions<sup>1</sup> and at high-temperature incineration/combustion conditions,<sup>2,3</sup> is reaction with hydroxyl (OH) free radicals. To accurately model halogenated hydrocarbon combustion, accurate semiempirical Arrhenius parameters describing rate behavior over extended temperature ranges are required. With the exception of our previous studies for saturated C<sub>1</sub> and C<sub>2</sub> chlorinated hydrocarbons<sup>4,5</sup> and our more recent studies of CHFCl<sub>2</sub>, CHF<sub>2</sub>Cl, and CH<sub>3</sub>CF<sub>2</sub>Cl,<sup>6,7</sup> previous measurements have only been reported over a narrow low-temperature range encompassing tropospheric

and stratospheric conditions.<sup>1</sup> At temperatures above 480 K, the prediction of rate constants for these compounds has been previously based solely on semiempirical transition-state theory (TST)<sup>8</sup> and structure/activity relationship (SAR) calculations.<sup>9</sup> Rate coefficient measurements over an extended temperature range are needed to verify and/or refine previously published TST and SAR models.

In this manuscript, we report high-precision rate coefficients for the reaction of OH with CH<sub>2</sub>ClCF<sub>2</sub>Cl ( $k_1$ ) and CH<sub>2</sub>ClCF<sub>3</sub> ( $k_2$ ) over an extended temperature range:



Significant curvature was observed in Arrhenius plots of the data. To provide a more accurate description of the experimental results, conventional TST calculations cast in the form  $k(T) = AT^B \exp(-C/T)$  were conducted where both  $A$  and  $B$  were calculated using TST and  $C$  was determined from a nonlinear least-squares fit to the experimental data. Ab initio calculations were used to define the activated complex. The TST-based modified Arrhenius expression is compared to previous TST and SAR predictions.

### Experimental Approach and Data Reduction

The experimental procedures were similar to our previous studies of OH reactions with CHFCl<sub>2</sub>, CHF<sub>2</sub>Cl, and CH<sub>3</sub>CF<sub>2</sub>Cl.<sup>6,7,10</sup> As a result, we only briefly summarize the procedures here.

\* To whom correspondence should be addressed. Phone: (937) 229-3604. Fax: (937) 229-2503. E-mail: Taylorph@udri.udayton.edu.

<sup>†</sup> Physical Optics Corporation.

<sup>‡</sup> University of Dayton Research Institute.

<sup>§</sup> Center for Computational Modeling of Nonstructural Materials.

OH radicals were produced by 193 nm photodissociation of HCFC/N<sub>2</sub>O/H<sub>2</sub>O/He gas mixtures with an ArF excimer laser (Questek model 2840). Initial OH concentrations, [OH]<sub>0</sub>, ranged from  $6 \times 10^9$  to  $2 \times 10^{10}$  molecules cm<sup>-3</sup> and were determined from the measured excimer laser fluence and published values of the N<sub>2</sub>O absorption coefficient ( $8.95 \times 10^{-20}$  cm<sup>2</sup> molecule<sup>-1</sup> at 298 K),<sup>11</sup> a photodissociation quantum yield for O(<sup>1</sup>D) production of unity,<sup>12</sup> and the rapid reaction of O(<sup>1</sup>D) with H<sub>2</sub>O (95% conversion in <20 μs). Experiments were typically conducted for photolysis energy fluences of 0.5 mJ cm<sup>-2</sup>. Following reaction initiation, time-resolved OH profiles were measured as functions of HCFC concentration using laser-induced fluorescence with a pulsed Nd:YAG pumped dye laser (Quanta Ray model DCR-1/PDL-2) emitting at the wavelength of 282.1 nm. The typical energy fluence was 200 μJ/pulse. Broadband fluorescence was collected at 309 nm using a PMT/band-pass-filter combination.

Four symmetrical ceramic heaters were used to provide isothermal conditions within the detection volume (reaction zone) of the optical reactor. The gas temperature was measured with a chromel/alumel thermocouple positioned ~2 mm from the probe intersection volume. Measurements using a second retractable chromel/alumel thermocouple indicated a variation of less than 3.5 K across the detection volume for gas temperatures ranging from 295 to 1000 K.

All experiments were carried out under slow flow conditions, and the buildup of reaction products was minimized. Individually controlled gas flows of HCFC/N<sub>2</sub>O/H<sub>2</sub>O/He were thoroughly mixed before entering the optical reactor. The composite flow conditioned the reactor for 5 min prior to the onset of data collection, thereby minimizing any effects due to reactant adsorption on the reactor walls. Flow rates were controlled with differential flow transducers, and the total volumetric flow rate just downstream of the reactor was measured before and after each experiment with a bubble meter. All experiments were conducted at a total pressure of  $740 \pm 10$  Torr. Stock samples of CH<sub>2</sub>ClCF<sub>2</sub>Cl and CH<sub>2</sub>ClCF<sub>3</sub> were obtained from PCR, Inc. Typically, 5–10 vol % of each stock sample was prepared in previously cleaned and dried 1 L (nominal) Pyrex bulbs at  $740 \pm 10$  Torr and introduced into the gas mixture and delivery system using a calibrated syringe pump (Sage Instruments, 341B). Initial concentrations varied from  $1 \times 10^{15}$  to  $1 \times 10^{16}$  molecule cm<sup>-3</sup> for CH<sub>2</sub>ClCF<sub>3</sub> and from  $5 \times 10^{14}$  to  $5.5 \times 10^{15}$  molecule cm<sup>-3</sup> for CH<sub>2</sub>ClCF<sub>2</sub>Cl.

Over the entire temperature range, reactive and diffusive OH radical decay profiles exhibited exponential behavior and were fit by the following nonlinear expression:

$$[\text{OH}] = [\text{OH}]_0 \exp(-k't) + \gamma \quad (1)$$

where  $\gamma$  is the constant background signal level and  $t$  is the time delay between the two lasers. Because [HCFC] > 1000-[OH] in all reactive experiments, exponential OH radical decays of the pseudo-first-order decay constant  $k' = k[\text{HCFC}] + k_d$  were observed.  $k_d$  is the first-order rate constant for OH radical disappearance from the probe volume due to diffusion and reaction with impurities in the carrier gas. The bimolecular rate constant,  $k$ , was obtained from the slope of the least-squares straight line through the plot of  $k'$  versus [HCFC], as illustrated for CH<sub>2</sub>ClCF<sub>2</sub>Cl in Figure 1.

Gas chromatography/mass spectrometry (GC/MS) analyses indicated that both HCFC substrates were free of contaminants (>99.9% pure). The remaining chemicals used in our gas delivery system had the following stated minimum purities: He

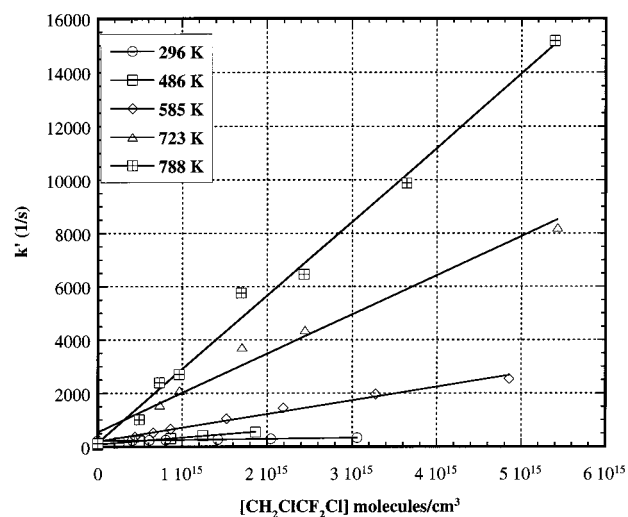


**Figure 1.** Plot of pseudo-first-order rate coefficient  $k'$  vs [CH<sub>2</sub>ClCF<sub>2</sub>Cl] for five reaction temperatures.

**TABLE 1: Absolute Rate Coefficients for  $k_1$ <sup>a</sup>**

temp (K)	$10^{14}k_1$ (cm <sup>3</sup> molecule <sup>-1</sup> s <sup>-1</sup> )	temp (K)	$10^{14}k_1$ (cm <sup>3</sup> molecule <sup>-1</sup> s <sup>-1</sup> )
295	1.84 ± 0.07	461	11.70 ± 0.37
309	2.27 ± 0.25	486	14.29 ± 0.57
320	2.86 ± 0.26	517	19.11 ± 0.78
335	3.83 ± 0.41	550	26.28 ± 1.55
347	4.07 ± 0.12	585	30.67 ± 0.64
363	4.62 ± 0.16	625	41.69 ± 2.12
378	5.95 ± 0.28	668	58.81 ± 3.54
398	6.52 ± 0.23	723	101.98 ± 3.53
418	7.93 ± 0.41	788	125.29 ± 12.37
439	10.07 ± 0.28		

<sup>a</sup> Errors represent  $\pm 2\sigma$ .

**TABLE 2: Absolute Rate Coefficients for  $k_2$ <sup>a</sup>**

temp (K)	$10^{14}k_1$ (cm <sup>3</sup> molecule <sup>-1</sup> s <sup>-1</sup> )	temp (K)	$10^{14}k_1$ (cm <sup>3</sup> molecule <sup>-1</sup> s <sup>-1</sup> )
295	1.76 ± 0.25	460	8.71 ± 0.27
309	2.17 ± 0.20	484	9.79 ± 0.36
319	2.58 ± 0.27	514	13.50 ± 0.32
334	3.28 ± 0.27	546	16.13 ± 0.38
347	3.77 ± 0.31	581	18.90 ± 0.37
362	3.91 ± 0.24	620	24.96 ± 0.88
378	4.39 ± 0.14	666	29.86 ± 1.25
396	5.33 ± 0.19	721	36.82 ± 2.60
415	6.22 ± 0.45	786	41.21 ± 3.28
438	7.23 ± 0.38	866	71.08 ± 2.49

<sup>a</sup> Errors represent  $\pm 2\sigma$ .

(99.999+); N<sub>2</sub>O (99.9%); H<sub>2</sub>O (HPLC organic-free reagent grade).

## Experimental Results

Absolute rate constants for  $k_1$  and  $k_2$  are presented in Tables 1 and 2, respectively. Random error limits ( $\pm 2\sigma$ ) derived from a propagation of error analysis ranged from 2% to 14% with a vast majority of the values less than 10%. The possibility that OH decays could be due to reaction with photolytically generated but unreacted O atoms was investigated by varying the H<sub>2</sub>O concentration. Bimolecular rate determinations were unaffected by 5-fold changes in [H<sub>2</sub>O], indicating that unreacted O atoms had no effect on the observed measurements. In the absence of reactant impurities, sources of systematic error were then limited to thermally and photolytically induced secondary reactions. The possibility of thermal artifacts was investigated

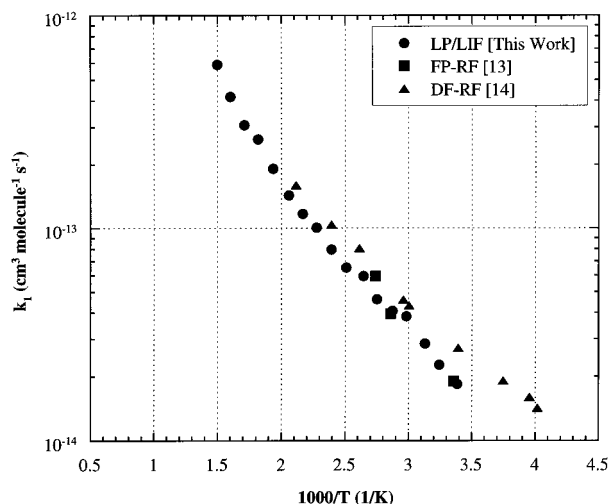


**Figure 2.** Arrhenius plot of experimental measurements for  $k_1$ . Also shown are prior experimental studies (delineated by the experimental method) at lower temperatures.<sup>13,14</sup>

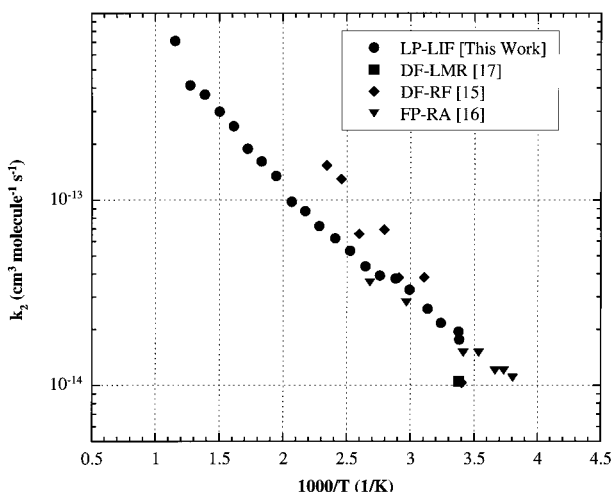


**Figure 3.** Arrhenius plot of experimental measurements for  $k_2$ . Also shown are prior experimental studies (delineated by the experimental method) at lower temperatures.<sup>15–17</sup>

by varying the total gas flow rate.  $k_1$  and  $k_2$  were found to be independent of residence time in the high-temperature region, implying a lack of thermal reaction of the substrates at the highest temperatures of these studies. The effect of laser photolysis on the substrate was observed to be insignificant on the basis of numerous experiments where a 5-fold variation of the excimer laser intensity (0.1–0.5 mJ cm<sup>-2</sup>) had no observable effect on OH decays.

As illustrated in Figures 2 and 3, to our knowledge, this is the first report of experimental measurements for these reactions above temperatures of 480 K. Also shown in Figures 2 and 3 are previous measurements at lower temperatures reported using different techniques.<sup>13–17</sup> Examination of the rate measurements for  $k_1$  indicates that our rate measurements were slightly smaller than those previously reported by Watson et al.<sup>13</sup> and Jeong et al.<sup>14</sup> The deviation, however, is within the estimated error limits for both studies. For  $k_2$ , our measurements above room temperature were substantially lower than those reported by Clyne and Holt<sup>15</sup> and slightly higher than those reported by Handwerk and Zellner.<sup>16</sup> In contrast, a previous room-temperature measurement by Howard and Evenson<sup>17</sup> and the room-temperature data of Clyne and Holt<sup>15</sup> are about 70% lower than our room-temperature measurements. The deviation between our

measurements and those of Handwerk and Zellner is within estimated error limits. A plausible reason for the discrepancy between our measurements and those using the discharge flow technique may be related to surface reactions or photolysis effects. Direct removal of OH on the wall is taken into account in the discharge flow data treatment. However, reaction of OH with adsorbed CH<sub>2</sub>ClCF<sub>3</sub> would give an erroneously high “gas-phase” rate coefficient. This rationale may partially explain the discrepancy between our data and the data of Clyne and Holt<sup>15</sup> at elevated temperatures. However, at room temperature, the discrepancy is in the opposite direction. This suggests that photolysis effects may be responsible. Our studies of possible photolysis effects were negative for photolysis intensities of <0.5 mJ cm<sup>-2</sup>. The generally good agreement of our measurements of  $k_1$  with previous discharge flow measurements<sup>14</sup> further suggests that photolysis effects are insignificant. A reasonable explanation for the scatter in the measurements of  $k_2$  is thus difficult to ascertain.

## Discussion

As illustrated in Figures 2 and 3, the Arrhenius plot for  $k_1$  and  $k_2$  demonstrated significant curvature, particularly above 500 K. Although the purely empirical fit is the best statistical representation of the data, we have previously shown that the magnitudes of  $A$ ,  $B$ , and  $C$  for these reactions are often theoretically implausible.<sup>6,7</sup> Consequently, a semiempirical fitting approach that provides physical insight into the thermodynamic properties of the respective transition states has been used. Our approach was to calculate  $A$  and  $B$  using conventional transition-state theory (TST) and then to determine  $C$  by an empirical fit to the three-parameter expression that has now been reduced to one variable. This approach was first demonstrated by Shaw<sup>18</sup> and Cohen<sup>19–21</sup> in TST calculations for the reactions of O atoms and OH radicals with alkanes and halogenated alkanes.

This approach was justified because  $A$  and  $B$  can be expressed in terms of the thermodynamic quantities  $\Delta C_p^\ddagger$  and  $\Delta S_p^\ddagger$ , which are relatively accurately calculable using TST (whereas  $C$  is related to  $\Delta H_p^\ddagger$ , which is not accurately calculable using TST). The weakness in this approach is that  $\Delta C_p^\ddagger, \text{vib}$  varies with temperature. However, changes in  $\Delta C_p^\ddagger, T$  decrease asymptotically with temperature, and this approach is reasonable for TST predictions at combustion temperatures. As shown below, a mean  $\Delta C_p^\ddagger, T$  value is used in these calculations. Following Shaw, we can show

$$A = (R'k/h)298^{(-\Delta C_p^\ddagger, T/R)} \exp[(\Delta S_p^\ddagger, 298\text{K} - \Delta C_p^\ddagger, T/R)] \quad (2)$$

$$B = 2 + (\Delta C_p^\ddagger, T)/R \quad (3)$$

$$C = (\Delta H_p^\ddagger, 298\text{K} - 298\Delta C_p^\ddagger, T/R) \quad (4)$$

where  $\Delta S_p^\ddagger, 298\text{K}$  is the entropy of activation at 298 K in pressure standard state,  $\Delta C_p^\ddagger, T$  is the heat capacity of activation at a specified temperature,  $\Delta H_p^\ddagger, 298\text{K}$  is the enthalpy of activation at 298 K in pressure standard state,  $R$  is the ideal gas constant in cal mol<sup>-1</sup> K<sup>-1</sup> units,  $R'$  is the ideal gas constant in L atm mol<sup>-1</sup> K<sup>-1</sup> units,  $k$  is the Boltzmann constant, and  $h$  is Planck's constant. The units of  $A$  are the same as  $k(T)$ , i.e., L mol<sup>-1</sup> s<sup>-1</sup>.

$\Delta S_p^\ddagger, 298\text{K}$  was previously calculated by Cohen and Benson<sup>8</sup> for  $k_1$  and  $k_2$  using the haloalkane reagent as the reference compound. They calculated a modified Arrhenius expression over a wide temperature range by combining TST calculations and curve-fitting schemes to the available low-temperature

experimental measurements. We have utilized the same general approach; however, ab initio calculations were used to provide a more accurate definition of the transition-state geometry.

The ab initio calculations were performed using the GAUSSIAN code<sup>22,23</sup> on Cray Y-MP, Cray C-90, HP-PARisk, and SGI Power-Challenge computers. First, the geometries of the reactants, transition state (TS), and products were optimized at the HF and MP2(FU) levels using the 6-31G(d) atomic basis set. Vibrational frequencies for the optimized structures were computed to evaluate the zero-point energies as well as to confirm the location of minima (no imaginary frequency) or TS (one imaginary frequency only). Single-point energy evaluations at the MP2 optimized geometries were used to obtain the G2(MP2) energy as proposed by Curtiss et al.<sup>24</sup> The G2(MP2) energies for the reactants, products, and transition state were computed by including the zero-point energies calculated at the HF level (using frequencies scaled by 0.8929). A summary of the ab initio optimized geometries and vibrational frequencies of the transition states for  $k_1$  and  $k_2$  can be found in ref 10.

Of the various corrections to the haloalkane model compound,  $\Delta_{\text{int rot}}$  was the largest and most difficult to estimate. In our previous studies of  $\text{CH}_3\text{CF}_2\text{Cl}$ ,<sup>7</sup> the hindered rotor model of Cohen and Benson<sup>8</sup> was found to be a reasonably accurate approximation for estimating the internal rotation changes at the transition state. The same result was observed for these two reactions. The Hartree–Fock and MP2 levels of theory resulted in values of  $\Delta S_p^\ddagger$  for  $k_1$  and  $k_2$  of  $-23.01$  and  $-26.17$   $\text{cal mol}^{-1} \text{K}^{-1}$  and  $-26.10$  and  $-28.53$   $\text{cal mol}^{-1} \text{K}^{-1}$ , respectively. The MP2 calculations were within 1–2 eu of the earlier calculations of Cohen and Benson<sup>8</sup> ( $-27.2$   $\text{cal mol}^{-1} \text{K}^{-1}$  for  $k_1$  and  $-27.0$   $\text{cal mol}^{-1} \text{K}^{-1}$  for  $k_2$ ). To evaluate the temperature exponent, we directly calculated an average  $\Delta C_p^\ddagger$  from 298 to 1000 K using the harmonic oscillator/rigid free rotor approximation with a correction for hindered internal rotation in the TS. The details of these calculations were given previously.<sup>6</sup> For  $k_1$ , the resulting mean  $\Delta C_p^\ddagger$  was  $-0.25R$  and  $0.1R$  for the Hartree–Fock and MP2 levels of theory, respectively. For  $k_2$ , the resulting mean  $\Delta C_p^\ddagger$  was  $-0.08R$  and  $-0.13R$  for the Hartree–Fock and MP2 levels of theory, respectively.

The best fit, TST-based modified Arrhenius expression, as determined from a minimization of the nonlinear least-squares error,  $\chi^2$ , for experimental measurements of  $k_1$  and  $k_2$  was observed to be the MP2 ab initio model and is given by the following expressions:

$$k_1(296-788 \text{ K}) = (8.53 \pm 4.06) \times 10^{-19} T^{2.28 \pm 0.18} \exp[(-937 \pm 296)/T] \text{ cm}^3 \text{ molecule}^{-1} \text{ s}^{-1}$$

$$k_2(296-866 \text{ K}) = (3.06 \pm 4.02) \times 10^{-18} T^{1.91 \pm 0.03} \exp[(-644 \pm 313)/T] \text{ cm}^3 \text{ molecule}^{-1} \text{ s}^{-1}$$

The uncertainty ( $\pm 2\sigma$ ) in the modified Arrhenius parameters is based primarily on a  $\pm 10\%$  uncertainty in the vibrational frequencies as discussed in detail in ref 6.

The best-fit TST-based modified Arrhenius expressions are plotted along with all of the available experimental data from stratospheric to near-combustion temperatures in Figures 4 and 5 for  $k_1$  and  $k_2$ , respectively. For  $k_1$ , the model is in good agreement ( $\pm 20\%$ ) with the measurements of Watson et al.<sup>13</sup> but significantly lower than the sub-room-temperature data of Jeong et al.<sup>14</sup> For  $k_2$ , the model is in good agreement ( $\pm 20\%$ ) with the measurements of Handwerk and Zellner<sup>16</sup> but significantly higher than the room-temperature data of Howard and

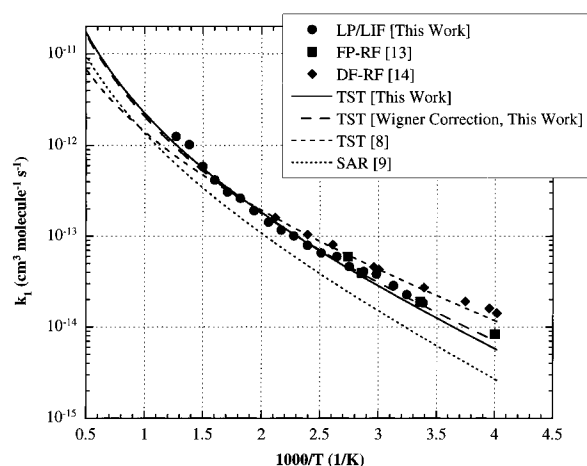


**Figure 4.** Arrhenius plot of experimental measurements for  $k_1$ . Also shown are TST calculations based on ab initio input calculations (MP2), TST calculations incorporating a Wigner tunneling factor, and previous TST<sup>8</sup> and SAR<sup>9</sup> calculations.

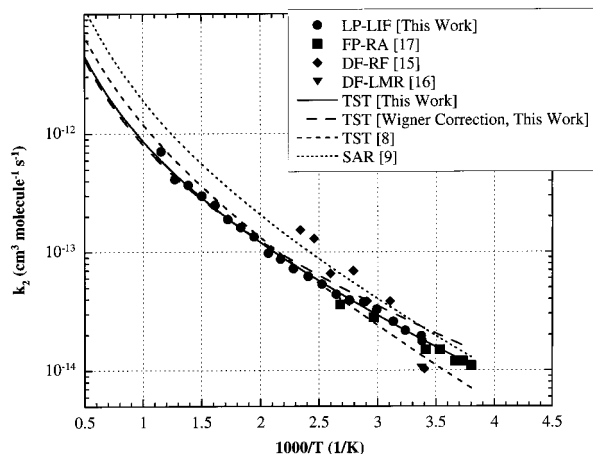


**Figure 5.** Arrhenius plot of experimental measurements for  $k_2$ . Also shown are TST calculations based on ab initio input calculations (MP2), TST calculations incorporating a Wigner tunneling factor, and previous TST<sup>8</sup> and SAR<sup>9</sup> calculations.

Evenson<sup>17</sup> and Clyne and Holt.<sup>15</sup> Given the scatter in the low-temperature data, the respective TST-based expressions accurately describe all of the available data within an uncertainty of about a factor of 2 and are recommended for use in kinetic modeling of the combustion and atmospheric reactions of  $k_1$  and  $k_2$ .

Comparisons of the new TST model with previous TST and SAR calculations are also shown in Figures 4 and 5. For  $k_1$ , reasonably good agreement ( $\pm$  a factor of 2) was observed between our TST model and the previous calculation of Cohen and Benson.<sup>8</sup> The Cohen and Benson calculation intersects our TST model at 575 K with predictions lying slightly below our expression at higher temperatures and slightly above our expression at lower temperatures. The SAR calculation<sup>9</sup> predicts lower rate measurements at all temperatures, with the deviation largest (greater than a factor of 2) below 400 K. For  $k_2$ , reasonably good agreement was once again observed between our TST expression and the previous calculation of Cohen and Benson. The Cohen and Benson calculation intersects our TST expression at 450 K with predictions lying slightly above our expression at higher temperatures and slightly below our expression at lower temperatures. The SAR calculation lies above our TST expression at all temperatures, with the deviation greater than a factor of 2 above 1000 K.

This study coupled with rate determinations for CHFCl<sub>2</sub> and CHF<sub>2</sub>Cl<sup>6</sup> suggests that room-temperature reactivity and transition-state enthalpy changes (derivable from eq 4) for C<sub>1</sub>- and C<sub>2</sub>-saturated HCFCs are primarily influenced by localized halogen substitution (at the reaction site). Room-temperature reactivity and transition-state enthalpy changes for *k*<sub>1</sub> and *k*<sub>2</sub> were very similar (TS enthalpy changes were 1329 and 1225 cal mol<sup>-1</sup> for *k*<sub>1</sub> and *k*<sub>2</sub>, respectively) and differ from the results obtained for CHFCl<sub>2</sub> and CHF<sub>2</sub>Cl (TS enthalpy changes were 1057 and 2173 cal mol<sup>-1</sup>, respectively). This suggests that changes in halogen substitution β to the reaction site have minimal impact on reactivity for this class of compounds.

**Notes Added in Proof.** At the request of one of the reviewers, a Wigner-based tunneling correction, Γ, has been applied to the data using the best available data for the imaginary frequency of the transition states. Schwartz et al.<sup>25</sup> have shown that our MP2/6-31G(d) ab initio calculations of the imaginary frequencies are inaccurate (~2440 cm<sup>-1</sup>). Schwartz et al.<sup>25</sup> calculated imaginary frequencies of CH<sub>3</sub>F<sub>y</sub> using G2 energies at various points along the MP2(full)/6-31G(D) IRC with a semiempirical Eckart function. As a result, we used the value of 1162 cm<sup>-1</sup> obtained for CH<sub>2</sub>CF<sub>2</sub> and applied it to both *k*<sub>1</sub> and *k*<sub>2</sub>. The magnitude of the tunneling correction varies from 2.3 to 1.1. The results are shown in Figures 4 and 5 for *k*<sub>1</sub> and *k*<sub>2</sub>, respectively. The tunneling correction improves the low-temperature TST fit for *k*<sub>1</sub> but overpredicts the low-temperature rate data for *k*<sub>2</sub>. The resulting modified Arrhenius expressions are

$$k_1(296-788 \text{ K}) = \Gamma(8.53 \pm 4.06) \times 10^{-19} T^{2.28 \pm 0.18} \exp[(-1156 \pm 365)/T] \text{ cm}^3 \text{ molecule}^{-1} \text{ s}^{-1}$$

$$k_2(296-866 \text{ K}) = \Gamma(3.06 \pm 4.02) \times 10^{-18} T^{1.91 \pm 0.03} \exp[(-822 \pm 399)/T] \text{ cm}^3 \text{ molecule}^{-1} \text{ s}^{-1}$$

**Acknowledgment.** T.F. and P.T. acknowledge support from the Environmental Protection Agency (Grant R819861-01-0). R.B. acknowledges the Air Force Office of Scientific Research and the Materials Directorate at Wright Laboratory for financial support and computational resources.

## References and Notes

- (1) Atkinson, R. *J. Phys. Chem. Ref. Data, Monogr.* **1989**, *1*.
- (2) Tsang, W. *Combust. Sci. Technol.* **1990**, *74*, 99.
- (3) Senkan, S. M. Survey of Rate Constants in the C/H/Cl/O System. In *Combustion Chemistry*, 2nd ed.; W. C. Gardiner, Jr., Ed., in press.
- (4) Jiang, Z.; Dellinger, B.; Taylor, P. H. *Int. J. Chem. Kinet.* **1993**, *25*, 9.
- (5) Jiang, Z.; Taylor, P. H.; Dellinger, B. *J. Phys. Chem.* **1993**, *97*, 550.
- (6) Fang, T. D.; Taylor, P. H.; Dellinger, B. *J. Phys. Chem.* **1996**, *100*, 4048.
- (7) Fang, T. D.; Taylor, P. H.; Dellinger, B.; Ehlers, C. J.; Berry, R. J. *J. Phys. Chem. A* **1997**, *101*, 5758.
- (8) Cohen, N.; Benson, S. W. *J. Phys. Chem.* **1987**, *91*, 162.
- (9) Atkinson, R. *Int. J. Chem. Kinet.* **1986**, *18*, 555.
- (10) Fang, T. D. Ph.D. Dissertation, University of Dayton, 1996.
- (11) Selwyb, G.; Podolske, J.; Johnston, H. S. *Geophys. Res. Lett.* **1977**, *4*, 427.
- (12) Simonaitis, R.; Heicklen, J. *J. Phys. Chem.* **1973**, *77*, 1932.
- (13) Watson, R. T.; Ravishankara, A. R.; Machado, G.; Wagner, S.; Davis, D. D. *Int. J. Chem. Kinet.* **1979**, *11*, 187.
- (14) Jeong, K.-M.; Hsu, K.-J.; Jeffries, J. B.; Kaufman, F. J. *Phys. Chem.* **1984**, *88*, 1222.
- (15) Clyne, M. A. A.; Holt, P. M. *J. Chem. Soc., Faraday Trans. 2* **1979**, *75*, 582.
- (16) Handwerk, V.; Zellner, R. *Ber. Bunsen-Ges. Phys. Chem.* **1978**, *82*, 1161.
- (17) Howard, C. J.; Evenson, K. M. *J. Chem. Phys.* **1976**, *64*, 4303.
- (18) Shaw, R. *J. Phys. Chem. Ref. Data* **1978**, *7*, 1179.
- (19) Cohen, N. *Int. J. Chem. Kinet.* **1982**, *14*, 1339.
- (20) Cohen, N. *Int. J. Chem. Kinet.* **1983**, *15*, 503.
- (21) Cohen, N. *Int. J. Chem. Kinet.* **1986**, *18*, 99.
- (22) Frisch, M. J.; Trucks, G. W.; Head-Gordon, M.; Gill, P. M. W.; Wong, M. W.; Foresman, J. B.; Johnson, B. G.; Schlegel, H. B.; Robb, M. A.; Replogle, E. S.; Gomperts, R.; Andres, J. L.; Raghavachari, K.; Binkley, J. S.; Gonzalez, C.; Martin, R. L.; Fox, D. J.; Defrees, D. J.; Baker, J.; Stewart, J. J. P.; Pople, J. A. *Gaussian 92*, revision F.4; Gaussian, Inc.: Pittsburgh, PA, 1992.
- (23) Frisch, M. J.; Trucks, G. W.; Schlegel, H. B.; Gill, P. M. W.; Johnson, B. G.; Robb, M. A.; Cheeseman, J. R.; Keith, T. A.; Petersson, G. A.; Montgomery, J. A.; Raghavachari, K.; Al-Laham, M. A.; Zakrzewski, V. G.; Ortiz, J. V.; Foresman, J. B.; Cioslowski, J.; Stefanov, B. B.; Nanayakkara, A.; Challacombe, M.; Peng, C. Y.; Ayala, P. Y.; Chen, W.; Wong, M. W.; Andres, J. L.; Replogle, E. S.; Gomperts, R.; Martin, R. L.; Fox, D. J.; Binkley, J. S.; Defrees, D. J.; Baker, J.; Stewart, J. P.; Head-Gordon, M.; Gonzalez, C.; Pople, J. A. *Gaussian 94*, revision A.1; Gaussian, Inc.: Pittsburgh, PA, 1995.
- (24) Curtiss, L. A.; Raghavachari, K.; Pople, J. A. *J. Chem. Phys.* **1993**, *98*, 1293.
- (25) Schwartz, M.; Marshall, P.; Berry, R. J.; Ehlers, C. J.; Petersson, G. A. *J. Phys. Chem. A* **1998**, *102*, 10074.